Published in final edited form as:
Am J Phys Anthropol. 2013 May ; 151(1): . doi:10.1002/ajpa.22255.

Trisomy 21 and Facial Developmental Instability

John M. Starbuck[1,*], **Theodore M. Cole III**[2], **Roger H. Reeves**[3], and **Joan T. Richtsmeier**[1,4]

[1]Department of Anthropology, The Pennsylvania State University, University Park, PA 16802

[2]Department of Basic Medical Science, School of Medicine, University of Missouri-Kansas City, Kansas City, MO 64108

[3]Department of Physiology and Institute for Genetic Medicine, Johns Hopkins University School of Medicine Baltimore, MD 21205

[4]Center for Functional Anatomy and Evolution, The Johns Hopkins University School of Medicine, Baltimore, MD 21205

Abstract

The most common live-born human aneuploidy is trisomy 21, which causes Down syndrome (DS). Dosage imbalance of genes on chromosome 21 (Hsa21) affects complex gene-regulatory interactions and alters development to produce a wide range of phenotypes, including characteristic facial dysmorphology. Little is known about how trisomy 21 alters craniofacial morphogenesis to create this characteristic appearance. Proponents of the "amplified developmental instability" hypothesis argue that trisomy 21 causes a generalized genetic imbalance that disrupts evolutionarily conserved developmental pathways by decreasing developmental homeostasis and precision throughout development. Based on this model, we test the hypothesis that DS faces exhibit increased developmental instability relative to euploid individuals. Developmental instability was assessed by a statistical analysis of fluctuating asymmetry. We compared the magnitude and patterns of fluctuating asymmetry among siblings using three-dimensional coordinate locations of 20 anatomic landmarks collected from facial surface reconstructions in four age-matched samples ranging from 4 to 12 years: 1) DS individuals (n=55); 2) biological siblings of DS individuals (n=55); 3) and 4) two samples of typically developing individuals (n=55 for each sample), who are euploid siblings and age-matched to the DS individuals and their euploid siblings (samples 1 and 2). Identification in the DS sample of facial prominences exhibiting increased fluctuating asymmetry during facial morphogenesis provides evidence for increased developmental instability in DS faces. We found the highest developmental instability in facial structures derived from the mandibular prominence and lowest in facial regions derived from the frontal prominence.

Keywords

Down syndrome; fluctuating asymmetry; craniofacial morphology; facial development; 3dMD

Since Darwin's publication of *The Origin of Species* in 1859, scientists have sought to understand how phenotypic variation arises within and between species. The study of both normal and abnormal ranges of phenotypic variation in humans is particularly interesting, given the potential for shedding light on human evolution, variation, and health.

[*]Correspondence to: Joan Richtsmeier, Department of Anthropology, The Pennsylvania State University, University Park, PA 16802. jta10@psu.edu.

Aneuploidies that are compatible with life provide a unique opportunity to address questions about how biological mechanisms of morphogenesis are altered by genetic and developmental perturbations. Trisomy 21 (i.e., Down syndrome) occurs in approximately 1:700 live births and is the most frequent liveborn human aneuploidy. Approximately 95% of Down syndrome (DS) cases occur from nondisjunction, which results in an entire extra copy of chromosome 21, although the specific alleles on the extra chromosome 21 differ for each individual (Fisher, 1983; Hassold et al., 1993). The other 5% of DS cases occur from mosaicism or translocation of chromosome 21, which may or may not produce strong phenotypic changes. DS has been argued to be an extreme form of copy number variation (Korbel et al., 2009; Wiseman et al., 2009; Ionita-Laza et al., 2009; Makino and McLysaght, 2010).

Gene-dosage imbalance caused by trisomy 21 (Kahlem et al., 2004; Birchler et al., 2005, 2007; Veitia et al., 2008) produces the clinical presentation of Down syndrome (DS), which includes impaired cognition, congenital heart anomalies, and characteristic facial dysmorphology (Jones, 2006; Reeves, 2001). In particular, craniofacial differences associated with DS include: brachycephaly, epicanthic folds, midfacial hypoplasia, poor or absent sinus development, flat or depressed nasal bridge, upturned nose, variable tooth morphogenesis and eruption patterns, reduced facial dimensions, and slower craniofacial growth rates (Kisling, 1966; Frostad et al., 1971; Jones, 2006; Megarbane et al., 2009). Our knowledge of how trisomy 21 alters developmental stability to produce the immediately recognizable and characteristic facial morphology typical of individuals with DS remains limited.

It has been hypothesized that trisomy 21 causes an “amplified developmental instability” (ADI) that results in asymmetry and increased variance of phenotypic characteristics (Shapiro, 1970, 1975, 1983; Barden, 1980; Townsend, 1983). Developmental instability (DI) refers to an organism's tendency to produce a morphological change in response to developmental perturbations (Richtsmeier et al., 2005). DI is the opposite of developmental stability, a term referring to the tendency of an organism not to exhibit morphological change when experiencing genetic or environmental perturbation due to canalization (*sensu* Waddington, 1957). Historically, developmental instability has been estimated as a measure of the metric differences between the left and right sides of symmetrically developing organisms. Typically, the left and right halves of a symmetric organism experience the same environmental and genomic influences during development. Consequently bilateral features of an organism (e.g., facial features) are expected to develop as replicates or mirror images of the opposite side. Genetic or environmental stress during development can increase developmental noise, expressed as minor departures from an ideal developmental program of perfect bilateral symmetry (Hallgrímsson et al., 2002). Stressors can potentially result in reduced developmental precision and increased DI during morphogenesis. Several studies have provided statistical evidence for a positive association between various types of stress and DI in a variety of traits in different populations and species (e.g., Livshits and Kobyliansky, 1991; Clarke, 1992; Naugler and Ludman, 1996; Willmore et al., 2005, 2006; DeLeon, 2007).

DI is frequently estimated in populations of normally symmetric organisms using an analysis of fluctuating asymmetry (FA) (Palmer and Strobeck, 1986, 1992, 2003; Palmer, 1994; Dongen, 2006). For a single measurement, we can define the (signed) asymmetry of an individual by subtracting the right-side measurement from the left: $L–R$. Three basic types of asymmetry (Fig. 1) are defined for samples based on frequency distributions of $L–R$: directional asymmetry, antisymmetry, and FA (Palmer and Strobeck, 1986, 1992, 2003; Palmer, 1994). Directional asymmetry describes a pattern of $L–R$ side differences that are biased towards a particular side with a unimodal distribution and a mean that is different

from zero. Antisymmetry describes a pattern of *L–R* side differences where consistent differences between sides are present but the differences are nondirectional, which results in a bimodal distribution and a mean of zero. Fluctuating asymmetries tend to be small and randomly distributed on each side of bilateral organisms (i.e., nondirectional), producing a distribution of *L–R* side values that is unimodal and centered at zero (Palmer and Strobeck, 1986; Richtsmeier et al., 2005). Several studies have shown that environmental and genetic effects can alter DA and FA (Barden, 1980; DeLeon, 2007; Klingenberg et al., 2010). It has been argued that FA can be measured as a surrogate to estimate DI (Palmer and Strobeck, 1986, 1992, 2003; Palmer, 1994; Dongen, 2006).

Proponents of the ADI hypothesis argue that trisomy 21 causes a generalized genetic imbalance that disrupts evolutionarily conserved developmental pathways by decreasing developmental homeostasis and precision (Shapiro, 1970, 1975, 1983). According to this model, the developmental program, which is under genetic control, is buffered or canalized in such a way that development tends to proceed along evolved trajectories unless perturbed by environmental or genetic insult (Shapiro, 1983). Proponents of the ADI hypothesis maintain that abnormal phenotypes found in individuals with DS (e.g., smaller palates, irregular tooth development, abnormal dermatoglyphics) tend to be the same as those that are less buffered (or canalized) during development in euploid individuals and, therefore, these traits are developmentally labile and more likely to exhibit increased phenotypic variation when perturbed by genetic or environmental insults during development (Shapiro, 1975, 1992). Several studies offer support for the ADI hypothesis (e.g., Shapiro et al., 1967, 1975; Cronk and Reed, 1981; Dunlap et al., 1986). Thus far, no studies have explored whether ADI is present in DS facial features.

The purpose of this investigation is to quantitatively determine if DS faces exhibit ADI relative to their euploid biological siblings and relative to typically developing, euploid siblings, unrelated to the DS sibling pairs. Because DI is difficult to measure in humans directly, we measure FA as a surrogate for DI and compare the amount of FA across samples of DS individuals, non-DS euploid siblings, and typically developing sibling pairs to determine how DI differs across samples. We hypothesize that DS individuals will exhibit increased or amplified facial DI as measured by FA, relative to both their own euploid biological siblings and to euploid non-biological sibling pairs. We use patterns of differences in FA to discuss how trisomy 21 can alter developmental stability during craniofacial morphogenesis.

Materials and Methods

Here we employ an age-matched, case-control, four-group study design (Fig. 2). Four cross-sectional samples of three-dimensional human facial images (4–12 yrs.) were acquired for analysis and are defined as follows: sample 1—DS individuals (N=55), sample 2—euploid individuals who are siblings of a DS individual (N=55), sample 3—euploid individuals who are part of a typically developing sibling pair and who are age-matched to sample 1 (N=55), and sample 4—euploid individuals who are part of a typically developing sibling pair that have a biological sibling in sample 3 and who are age-matched to sample 2 (N=55). Individuals in sample 1 were previously diagnosed with DS by medical practitioners. The parents of DS individuals were asked to report whether DS occurred from nondisjunction, mosaicism, or translocation at the time of image acquisition and by mail using a follow-up questionnaire. DS cases from mosaicism and translocation are rare (5%), and we have made efforts to exclude individuals with these diagnoses from the current study to focus on DS from nondisjunction; however, it is possible that individuals were included in this study who have DS from mosaicism or translocation. Sex ratios between age-matched samples are similar, but not equal (sample 1: 45% male, 55% female; sample 2: 53% male, 47% female;

sample 3: 38% male, 62% female; sample 4: 58% male, 42% female). No attempt was made to control for ethnic/ancestral background; however, the majority of the sample is Caucasian. All images used in this study were collected with protocols approved by the Pennsylvania State University Institutional Review Board (IRB # 23283 and # 36627).

Three-dimensional images of facial morphology were acquired using the 3dMD photogrammatic system (available at: http://3dmd.com/) after instructing subjects to display a neutral facial expression white sitting in an upright position. The 3dMD camera system is portable and acquires images simultaneously using six cameras, each with a different viewpoint, and merges them into a single, three-dimensional surface. The 3dMDpatient software (v4.0) was used to record the three-dimensional coordinates of 20 standard facial landmarks from each surface twice (Fig. 3). Several studies have confirmed that 3dMD surfaces are accurate three-dimensional representation of facial topography and that the three-dimensional locations of anatomical landmarks recorded from these surfaces are precise and reliable (Aldridge et al., 2005; Weinberg, 2006; Wong et al., 2008). Measurement error was assessed by collecting landmarks from images of five random individuals drawn from the overall sample. Each of these images was landmarked on five separate occasions with at least 24 h between landmarking sessions to avoid memory bias in landmark placement. Standard deviations of landmark coordinates along the *x*, *y*, and *z* axes were averaged to calculate mean measurement error (Valeri et al., 1998; Aldridge et al., 2005; Schmidt et al., 2011). Mean measurement error local to each landmark was estimated to be 0.29 mm (0.26 mm along the *x*-dimension, 0.30 mm along the *y*-dimension, and 0.31 mm along the *z*-dimension) and is considered adequately low for the purposes of this study. For each individual, we checked for gross landmark errors in data collection (e.g., mislabeling right and left side landmarks) by subtracting the coordinates of each landmarking trial from each other and confirming that differences were negligible. Landmark coordinates were then averaged from two separate digitizing episodes to further minimize any potential effects of measurement error for each individual. Average coordinate locations of landmarks were used for analyses.

Landmark coordinates were initially subjected to a Procrustes superimposition and principal components analysis (PCA) using MorphoJ software (Klingenberg, 2011) to determine whether or not males and females exhibit strong DA and FA differences in multidimensional shapespace. For both the symmetric and asymmetric components of shape variation, males and females from all samples completely overlap on PCA scatterplots for all principal component axes (Supporting Information Fig. 1), suggesting that strong differences in DA and FA are not present between 4- and 12-year-old males and females in our samples, despite the fact that sex ratios in each sample are not precisely the same.

We used a two-sample Euclidean Distance Matrix Analysis (EDMA) approach (Cole 2001) to statistically evaluate differences in FA between the following samples: 1) DS individuals (sample 1) versus their unaffected siblings (sample 2); and 2) typical individuals age-matched to the Down syndrome individuals (sample 3) versus their unaffected siblings (sample 4) who are age-matched to sample 2. Landmark data were used to compute 63 bilateral linear distances, and FA was estimated for each pair of distances. For each individual, the asymmetry of each measurement was quantified by subtracting the right side measurement from the left side measurement ($L–R$). A difference of 0 indicates perfect symmetry, while a positive value indicates a larger left-side measurement, and a negative value indicates a larger right-side measurement. The $L–R$ difference measures asymmetry without taking size differences between individuals into account. To account for potential size variation among individuals being compared in this study, we also quantified asymmetry using the natural logarithm of the ratio of L to R ($ln(L/R)$). This measure of asymmetry is scale-free (Palmer and Strobeck, 2003). While our samples are age-matched,

thereby reducing the need for a scale adjustment, by calculating asymmetry using both methods, we can evaluate the effect that size variation has on our results.

In some applications, it may be necessary to account for directional asymmetry (DA) when defining FA. DA is the mean of the (signed) asymmetries for the sample: $\mathrm{DA}=\overline{(L-R)}$. We can then redefine the asymmetry of an individual conditional on the amount of DA in the sample: $|(L-R)-DA|=|(L-R)-\overline{(L-R)}|$. The amount of fluctuating asymmetry in the sample is then the mean of A|*DA*. Noting that our measurement of FA is conditional on DA, we write $FA|DA=\overline{A|DA}=\overline{|(L-R)-\overline{(L-R)}|}$. The inclusion of DA in the definition of FA is common in studies that partition the variance in asymmetry into different components (e.g., Procrustes superimposition; Klingenberg and McIntyre, 1998; Klingenberg et al., 2002). However, it is not an essential part of FA as we study it here, and Richtsmeier et al. (2005) have argued that DA should only be considered when there is a good biological reason for doing so. Because we have no a priori reason to suspect DA is present in the human faces studied, the results presented in this paper have not been corrected for DA. However, it is noteworthy to mention that the results with a DA correction are similar to results presented here (Supporting Information Fig. 2).

For each linear distance, we consider the null hypothesis that the amount of FA is the same in the two samples we compare. For example, in a comparison of DS individuals with their unaffected siblings (Sib): H_0: $\mathrm{FA_{DS}}=\mathrm{FA_{Sib}}$. To test this hypothesis we define a test statistic $\mathrm{FA_{Diff}}=\mathrm{FA_{DS}}-\mathrm{FA_{Sib}}$. If the null hypothesis of equal FA is true, we expect $\mathrm{FA_{Diff}}=0$. If $\mathrm{FA_{Diff}}$ is greater than 0, the DS sample has more FA than the sample of their siblings for that particular measurement; if the difference is less than 0, the euploid sibling sample has more FA. We use the bootstrap to compute a marginal confidence interval for $\mathrm{FA_{Diff}}$ for each distance (Efron and Tibshirani, 1993; Davison and Hinkley, 1997). The algorithm is similar to the one developed by Richtsmeier et al. (2005), with a modification to account for the fact that individuals in two samples are related. Continuing with a comparison of the DS sample with their siblings:

1. Compute the test statistic. Call the sample sizes for the DS and sibling samples *n* (the same for both samples, since we have sibling pairs). Compute FA for both samples, defining FA as either $\overline{(L-R)}$ or $\overline{|\mathrm{ln}(\frac{L}{R})|}$. Define the empirical test statistic for the difference in FA: $\mathrm{FA_{Diff}}=\mathrm{FA_{DS}}$ - $\mathrm{FA_{Sib}}$. This is done for each linear distance;
2. Compute the bootstrap estimate of the test statistic. Select *n* DS-sibling pairs from the two samples, randomly and with replacement. Note that a given DS individual and his/her sibling are sampled together. Here is the difference between this application of the bootstrap and the algorithm in Richtsmeier et al. (2005). Call the pseudosample of DS individuals DS*; similarly, call the pseudosample of siblings Sib*. Using the respective pseudosamples, compute bootstrap estimates of FA, called $\mathrm{FA_{DS}}$* and $\mathrm{FA_{Sib}}$*. The bootstrap estimate for their difference is $\mathrm{FA_{Diff}}$*. Compute $\mathrm{FA_{Diff}}$* for each linear distance;
3. Conduct the bootstrap resampling. Repeat Step 2 *M* times, where *M* is some large number (e.g., 1,000 or more), independently generating new pseudosamples each time. For every resampling, compute a new estimate of $\mathrm{FA_{Diff}}$* and save it to an array. Again, there is an estimate for each distance;
4. For each distance, determine the marginal confidence interval from the bootstrap sample. Sort the array of $\mathrm{FA_{Diff}}$* estimates from smallest to largest: $\mathrm{FA_{Diff}}$*[1]… $\mathrm{FA_{Diff}}$*[*M*]. This vector is truncated to get a percentile confidence interval for

FA_{Diff} (i.e., the original estimate and not a bootstrap estimate). For a (1−α)% confidence interval, the lower bound will be FA_{Diff}*[(*M*)(α/2)] and the upper bound will be FA_{Diff}*[(*M*)(1−α/2)]. For example, if we want 90% confidence intervals (α=0.10) based on *M*=1,000 resamples, the lower and upper bounds will be FA_{Diff}*[50] and FA_{Diff}*[950], respectively.

5. Evaluate the null hypothesis using the confidence interval. To evaluate the null hypothesis, we see if the confidence interval for a given measurement contains 0, which is our expectation for FA_{Diff}. If the confidence interval excludes 0, the null is rejected for that linear distance, and the levels of FA in the two samples are considered to be different for that linear distance.

Additionally, we explored spatial patterning of FA differences between the DS sample and their siblings (i.e., samples 1 and 2), and the two typically developing sibling samples (i.e., samples 3 and 4) using an approach specific to human facial development. Differences in FA found between samples 3 and 4 provide an expectation of the types of differences that occur between biological siblings. The human face initially develops from five facial prominences that form during craniofacial morphogenesis: the frontonasal prominence, paired maxillary prominences, and paired mandibular prominences. Paired lateral and medial nasal prominences then form on the ventrolateral margin of the frontonasal prominence, and the paired mandibular prominences fuse. Around the eighth week of development, the facial prominences have migrated and merged and are arranged in a configuration similar to that found in fully-developed human faces. Based on this facial configuration, we divided the face into different regions representing the prominences that give rise to each facial region during craniofacial morphogenesis (Fig. 4). The face was divided into the following prominences: 1) frontal; 2) medial nasal (paired); 3) lateral nasal (paired); 4) maxillary (paired); and 5) mandibular. We assessed relative facial developmental stability in the DS sibling sample by exploring how frequently linear distances with significantly different FA were found within each developmental region. Linear distances exhibiting significantly different FA in each two-sample comparison were scored by tracking which developmental modules (i.e., prominences) each linear distance crosses. This was done for each linear distance exhibiting significantly different FA between each two-sample comparison. Because linear distances exhibiting significantly different FA between samples 3 and 4 provide an expectation of the quantity and types of FA we expect to differ between siblings, we subtracted the number of times each of these linear distances crossed each developmental boundary from the number of differences found between sample 1 and 2 to provide a summary of how FA between DS siblings (one trisomic and one euploid) differ from euploid siblings (both euploid). For each facial region, we then divided the number of times each linear distance exhibiting significantly different FA crossed each facial region by the number of times all possible linear distances could have crossed each facial region.

Results

In the comparison of DS individuals and their unaffected siblings, with FA defined as $|\overline{(L-R)}|$, 35 of the 63 linear distances (56%) exhibit significantly different FA on the basis of 90% confidence intervals for FA_{Diff} (Fig. 4A). In every significant case, the amount of FA is greater in the DS sample, with mean values of the amount of FA in the DS sample being 52% greater (Table 1). When FA is defined to account for possible differences in size $(\mathrm{FA}=\overline{|\ln(\frac{L}{R})|})$, the number of significant differences between the DS and unaffected sibling samples increases to 48 of 63 (76%) (Fig. 4B). Again, in every significant case, the amount of FA is greater in the DS sample, with mean values of the amount of FA in the DS sample

being 64% greater. Given the age and size variation in each sample, the results from the second bootstrap analysis ($ln(L/R)$) are likely more robust, since that definition of asymmetry is scale-invariant (Palmer and Strobeck, 2003).

In contrast to the comparison with DS individuals and their siblings, there were few significant differences in FA between the unrelated, typical individuals that were age-matched to the DS sample and their unaffected siblings. When FA was defined as $|\overline{(L-R)}|$, only 13 of 63 linear distances (21%) exhibited significantly different FA (Fig. 4C). When the test statistic accounts for differences in size $(\mathrm{FA}=|\overline{\ln(\frac{L}{R})}|)$, only seven linear distances (11%) exhibited significant differences in FA between the typical siblings (Fig. 4D).

Spatial patterning and FA results are similar for each bootstrap analysis (Table 2). For the FA difference $\overline{(L-R)}$ analysis, the mandibular prominence exhibits the greatest amount of FA and therefore DI, followed by the maxillary prominences, medial nasal prominences, lateral nasal prominences, and the frontal prominence. For the FA ratio $(\overline{|\ln(\frac{L}{R})|})$ analysis, the mandibular prominence again exhibits the greatest amount of FA and therefore DI, followed by the maxillary prominences, lateral nasal prominences, medial nasal prominences, and the frontal prominence. The main difference between patterns of differences for each analysis is the relative importance of the medial and lateral nasal prominences relative to the other facial prominences.

Discussion

Studies of normal and abnormal variation contribute to holistic and integrative anthropological approaches of understanding all aspects of the human condition. Chromosomal changes that are compatible with life hold the potential to alter developmental mechanisms and patterns of phenotypic variation, and consequently provide researchers with a unique opportunity to address questions about how biological mechanisms of development are altered by genetic and other perturbations.

We estimated patterns of fluctuating asymmetry (FA) in age-matched samples of DS individuals, siblings of individuals with DS, and samples of typically developing siblings and used statistical approaches to test for differences in facial FA to reveal differences in patterns of developmental instability (DI) in the face. The four sample sibling study design employed here allows the estimation of DI caused by trisomy 21 and gene-dosage imbalance relative to similar and dissimilar euploid backgrounds. Using two different measures of FA, we found that DS faces exhibit 140–164% more FA than the faces of their biological siblings and unrelated euploid individuals (i.e., samples 2–4) for the 63 bilateral linear distances evaluated (Table 1). Importantly, every linear distance exhibiting significantly different FA between samples displayed a larger magnitude of FA in the DS sample for each analysis. These results support the hypothesis of amplified DI in the faces of individuals with trisomy 21.

The outcomes of the two-sample comparisons illustrate that differences in FA between DS siblings reveal a 2.7-to 6.9-fold increase in the number of significant differences when compared with a comparison of FA in typical siblings (Fig. 4). Since FA corresponds to DI, linear distances exhibiting significantly different FA in the DS sample allow us to characterize the DI of different facial regions. Based on our analysis of DI in non-DS typical siblings, a comparison of the DI between DS sibling pairs reveals a graded difference in the effects of trisomy 21 on facial regions defined by developmental precursors (Fig. 4). The differences in DI enable a characterization of developmental regions of the DS face from the

most developmentally unstable to the most developmentally stable: mandibular prominence, maxillary prominences, medial nasal prominence, lateral nasal prominence, and the frontal prominence (see Table 2). Thus, in cases of trisomy 21, the frontal prominence gives rise to the most developmentally stable facial region, whereas the mandibular prominence gives rise to the least developmentally stable facial region.

According to the “amplified developmental instability” (ADI) model put forth by Shapiro (1975, 1983), trisomy 21 disrupts developmental homeostasis and causes generalized disturbances to developmental events that result in ADI. We found that DS facial morphology exhibits increased DI relative to biological siblings and unrelated euploid siblings, which supports Shapiro's contention that trisomy 21 results in ADI (Shapiro, 1975, 1983). However, our results indicate that facial regions derived from embryonic facial prominences are affected differentially by gene-dosage imbalance caused by trisomy 21. This result contradicts the aspect of Shapiro's ADI hypothesis arguing that trisomy causes a “generalized” disruption to development (Shapiro, 1975, 1983).

Because of differences in age-range, syndromic status, methodology, landmark choice, and the facial developmental interpretative framework employed here, our results are difficult to compare to other studies of facial asymmetry. In particular, landmark choice is often influenced by multiple factors such as repeatability, image type, and image quality. For example, some soft-tissue landmarks are determined by palpation or by using the underlying bony anatomy of the skull to determine landmark placement. The 3dMD images capture a 180° surface image of the soft-tissue of the face and oftentimes regions around the forehead and ears are obscured by hair, thereby limiting the number of anatomical landmarks collectable from these regions.

Several other morphometric studies have found different types of asymmetry in human faces using anatomical landmarks, semi-landmarks, and spatially-dense quasilandmarks; however, the types and locations of asymmetries found are dependent on the craniofacial condition being investigated and the methodology employed (Hammond et al., 2008; Klingenberg et al., 2010; Claes et al., 2011, 2012). In a recent study using spatially-dense quasi-landmarks and healthy controls, researchers found that the middle and lower thirds of the face express more asymmetry (DA and FA were not studied separately) than the upper face (Claes et al., 2011). Although the current study focuses on facial FA in an aneuploid population using a developmental interpretative framework, the facial asymmetry results from Claes et al. (2011) are comparable to the results presented here for children with DS. However, trisomy 21 likely exaggerates asymmetry differences typically found in the lower and middle thirds of the face of euploid populations.

Facial development involves a series of highly coordinated spatiotemporal morphogenetic events that include the correct formation, expansion, and fusion of facial prominences (Jiang et al., 2006; Brugmann et al., 2006; Feng et al., 2009). Tissues of the craniofacial complex are primarily derived from pluripotent and transiently migratory cranial neural crest cells, which originate from the dorsal aspect of the neural tube during embryogenesis (Cordero et al., 2010). Unique molecular programs are employed in each facial prominence throughout craniofacial development (Feng et al., 2009). Previous studies using animal models have identified many important tissue interactions and molecular mechanisms that contribute to facial morphogenesis, including individual genes and signaling pathways (e.g., Shh, Fgf's, Bmp's, Wnt's, Dlx, Msx, Otx) and signaling centers (e.g., Frontonasal Ectodermal Zone—FEZ, nasal pit), which all play important roles in the formation of craniofacial phenotypes (Hu and Helms, 1999; Hu et al., 2003; Helms et al., 2005; Brugmann et al., 2006; Brugmann et al., 2007; Szabo-Rogers et al., 2008; Hu and Marcucio, 2009a,b; Liu et al., 2010; Young

et al., 2010). However, we still lack a clear understanding of the gene networks that regulate face formation (Chai and Maxson, 2006).

Subtle changes to any of the biological processes of craniofacial morphogenesis due to gene dosage imbalance caused by trisomy 21 could potentially affect developmental stability, prominence formation, and facial development to produce craniofacial phenotypes associated with DS. Exactly how gene-dosage imbalance from trisomy 21 alters developmental stability and facial morphogenesis is unknown; however, there are many ways that the DS facial phenotype could arise developmentally:

1. Trisomy 21 may affect the spatiotemporal deployment of important genes expressed in the developing facial primordia through complex regulatory mechanisms. In particular, growth factors of the Wnt, Bmp, and Fgf families and their stoichiometric interactions play important roles in shaping the maxillary and mandibular prominences (Foppiana et al. 2007; Marcucio et al. 2005). Since our results suggest that the mandibular and maxillary prominences are more affected than other prominences, it is possible that trisomy 21 alters facial gene expression, possibly through *cis*- or *trans*-misregulation caused by gene-dosage imbalance;

2. Trisomy 21 may affect cranial neural crest cells by inhibiting their delamination and migration from the rhombomeres into pharyngeal arches 1 and 2 or by interfering with cell type specification and apoptosis. There is evidence from Ts65Dn DS mouse models that trisomy 21 acts as a neurocristopathogen, resulting in reduction of mitosis, proliferation, and migration of cranial neural crest cells into the face during craniofacial morphogenesis (Roper et al., 2009). Deficiencies in bone formation have been found in DS mouse models, such as lower bone mineral density for trabecular and cortical bone and lower bone volume fraction and fewer rod-like trabeculae (Blazek et al., 2010; Parsons et al., 2007), which suggests that gene-dosage imbalance results in reduced osteoblast and odontoblast activity and ultimately contributes to the unique facial morphology found in DS. Additionally, Meckel's cartilage forms from neural crest cells derived from the first pharyngeal arch and acts as a template around which membrane bone is laid down to form the mandible (Wyganowska-Świątkowska and Przystańska, 2011). It is possible that gene-dosage imbalance impairs morphogenesis of Meckel's cartilage, possibly by impairing the spatiotemporal migration of neural crest cells and disrupting conversion of cartilage to bone;

3. Additionally, gene-dosage imbalance caused by trisomy 21 may be changing the boundaries of developing facial regions, possibly by changing growth rates of particular prominences (e.g., the mandibular prominence) or by reducing the amount of time prominences are in contact before fusion occurs. Our results could support this hypothesis because linear distances exhibiting significant differences in FA between DS siblings tend to cross boundaries between developmental modules, rather than being contained within modules (Fig. 4A,B).

This list is by no means exhaustive and our results do not exclude any of the proposed mechanisms. If similar patterns of DI are found using mouse models for Down syndrome (Rueda et al., 2012) these mechanisms can be tested in developing organisms. Such an approach could eventually lead to a better understanding of the effects of gene-dosage imbalance upon craniofacial morphogenesis and to treatments designed to alleviate health disparities associated with the face and skull in DS (e.g., reduced facial dimensions, midfacial hypoplasia, irregular sinus development, abnormal tooth morphogenesis, malocclusion, etc.).

The results from this investigation are particularly interesting for anthropologists who study craniofacial variation. Throughout human evolution, different regions of the craniofacial complex have changed in shape and size due to genetic and environmental changes, speciation events, and cultural/behavioral adaptations related to dietary change. Previously, Shapiro (1975, 1983) argued that the phenotypic characteristics most often perturbed in DS are the same phenotypic characteristics that are more developmentally labile in euploid populations. It may be the case that facial primordia giving rise to the mandibular and maxillary regions of the face are more developmentally plastic than other regions of the face. On a developmental scale, these results help us understand how trisomy 21 alters the typical human facial blueprint to produce the characteristic facial appearance associated with DS. However, on an evolutionary scale these results suggest that the mandibular and maxillary regions of human faces exhibit more developmental plasticity than other regions of the face. Considering the range of anatomical variation associated with the mandibular and maxillary regions of the face across mammals, it is possible that these particular facial regions are more developmentally labile and capable of responding to the demands of natural selection.

Supplementary Material

Refer to Web version on PubMed Central for supplementary material.

Acknowledgments

Additional Supporting Information may be found in the online version of this article.

Grant sponsor: National Institute of Child Health & Human Development (NICHHD)/NIH; Grant number: R01-HD038384 (to R.H.R.); Grant sponsor: National Institute of Dental and Craniofacial Development NIDCR/NIH; Grant numbers: R01-DE018500, R01-DE018500-S2, ARRA 3R01DE018500-02S1, and R01-DE022988 (to J.T.R.); Grant sponsor: Graduate Research Fellowship grant from the National Science Foundation; Grant number: DGE-053135 (to J.M.S.); Grant sponsor: Doctoral Dissertation Research Improvement Grant from the National Science Foundation; Grant number: BCS-1061563 (to J.M.S.).

Literature Cited

Aldridge K, Boyadjiev SA, Capone GT, DeLeon VB, Richtsmeier JT. Precision and error of three-dimensional phenotypic measures acquired from 3dMD photogrammetric images. Am J Med Genet A. 2005; 138:247–253. [PubMed: 16158436]

Barden HS. Fluctuating dental asymmetry: a measure of developmental instability in Down syndrome. Am J Phys Anthropol. 1980; 52:169–173. [PubMed: 6445164]

Birchler JA, Riddle NC, Auger DL, Veitia RA. Dosage balance in gene regulation: biological implications. Trends Genet. 2005; 21:219–226. [PubMed: 15797617]

Birchler JA, Yao H, Chudalayandi S. Biological consequences of dosage dependent gene regulatory systems. Biochim Biophys Acta. 2007; 1769:422–428. [PubMed: 17276527]

Blazek JD, Billingsley CN, Newbauer A, Roper RJ. Embryonic and not maternal trisomy causes developmental attenuation in the Ts65Dn mouse model for Down syndrome. Dev Dyn. 2010; 239:1645–1653. [PubMed: 20503361]

Brugmann SA, Tapadia MD, Helms J. The molecular origins of species-specific facial pattern. Curr Top Dev Biol. 2006; 73:1–42. [PubMed: 16782454]

Brugmann SA, Kim J, Helms J. Looking different: understanding diversity in facial form. Am J Med Genet A. 2006; 140:2521–2529. [PubMed: 16838331]

Brugmann SA, Goodnough LH, Gregorieff A, Leucht P, ten Berge D, Fuerer C, Clevers H, Nusse R, Helms J. Wnt signaling mediates regional specification in the vertebrate face. Development. 2007; 134:3283–3295. [PubMed: 17699607]

Chai Y, Maxson RE Jr. Recent advances in craniofacial morphogenesis. Dev Dyn. 2006; 235:2353–2375. [PubMed: 16680722]

Claes P, Walters M, Vandermeulen D, Clement JG. Spatially-dense 3D facial asymmetry assessment in both typical and disordered growth. J Anat. 2011; 219:444–455. [PubMed: 21740426]

Claes P, Walters M, Shriver MD, Puts DA, Gibson G, Clement JG, Baynam G, Verbeke G, Vandermeulen D, Suetens P. Sexual dimorphism in multiple aspects of 3D facial symmetry and asymmetry defined by spatially-dense geometric morphometrics. J Anat. 2012; 221:97–114. [PubMed: 22702244]

Clarke G. Fluctuating asymmetry: a technique for measuring developmental stress of genetic and environmental origin. Acta Zool Fennica. 1992; 191:34–35.

Cole, TM, III. Further applications of EDMA. In: Lele, S.; Richtsmeier, J., editors. An invariant approach to statistical analysis of shapes. Boca Raton: Chapman and Hall/CRC; 2001. p. 263-284.

Cordero DR, Brugmann S, Chu Y, Bajpai R, Jame M, Helms JA. Cranial neural crest cells on the move: their roles in craniofacial development. Am J Med Genet A. 2010; 155:270–279. [PubMed: 21271641]

Cronk CE, Reed RB. Canalization of growth in Down syndrome children three months to six years. Hum Biol. 1981; 53:383–398. [PubMed: 6458549]

Davison, AC.; Hinkley, DV. Bootstrap methods and their applications. Cambridge: Cambridge University Press; 1997.

DeLeon VB. Fluctuating asymmetry and stress in a medieval Nubian population. Am J Phys Anthropol. 2007; 132:520–534. [PubMed: 17243154]

Dongen SV. Fluctuating asymmetry and developmental instability in evolutionary biology: past, present and future. J Evol Biol. 2006; 19:1727–1743. [PubMed: 17040371]

Dunlap SS, Aziz MA, Rosenbaum KN. Comparative anatomical analysis of human trisomies 13, 18, and 21: I. The forelimb. Teratology. 1986; 33:159–186. [PubMed: 2943045]

Efron, B.; Tibshirani, R. An introduction to the bootstrap. New York: Chapman and Hall; 1993.

Feng W, Leach SM, Tipney H, Phang T, Geraci M, Spritz RA, Hunter LE, Williams T. Spatial and temporal analysis of gene expression during growth and fusion of the mouse facial prominences. PLoS One. 2009; 4:1–31.

Fisher WL. Quantitative and qualitative characteristics of the face in Down's syndrome. J Michigan Dent Assoc. 1983; 65:105–107.

Foppiana S, Hu D, Marcucio RS. Signaling by bone morphogenetic proteins directs formation of an ectodermal signaling center that regulated craniofacial development. Dev Biol. 2007; 312:103–114. [PubMed: 18028903]

Frostad WA, Cleall JF, Melosky LC. Craniofacial complex in the trisomy 21 syndrome (Down's syndrome). Arch Oral Biol. 1971; 16:707–722. [PubMed: 4254102]

Hallgrímsson B, Willmore K, Hall BK. Canalization, developmental stability, and morphological integration in primate limbs. Am J Phys Anthropol Suppl. 2002; 35:131–158.

Hammond P, Forster-Gibson C, Chudley AE, Allanson JE, Hutton TJ, Farrell SA, McKenzie J, Holden JJA, Lewis MES. Face-brain asymmetry in autism spectrum disorders. Mol Psychiatr. 2008; 13:614–623.

Hassold T, Hunt PA, Sherman S. Trisomy in humans: incidence, origin and etiology. Curr Opin Genet Dev. 1993; 3:398–403. [PubMed: 8353412]

Helms J, Cordero D, Tapadia MD. New insights into craniofacial morphogenesis. Development. 2005; 132:851–861. [PubMed: 15705856]

Hu D, Helms J. The role of Sonic hedgehog in normal and abnormal craniofacial morphogenesis. Development. 1999; 126:4873–4884. [PubMed: 10518503]

Hu D, Marcucio RS, Helms J. A zone of frontonasal ectoderm regulates patterning and growth in the face. Development. 2003; 130:1749–1758. [PubMed: 12642481]

Hu D, Marcucio RS. Unique organization of the frontonasal ectodermal zone in birds and mammals. Dev Biol. 2009; 325:200–210. [PubMed: 19013147]

Hu D, Marcucio RS. A SHH-responsive signaling center in the forebrain regulates craniofacial morphogenesis via the facial ectoderm. Development. 2009; 136:107–116. [PubMed: 19036802]

Ionita-Laza I, Rogers AJ, Lange C, Raby BA, Lee C. Genetic association analysis of copy-number variation (CNV) in human disease pathogenesis. Genomics. 2009; 93:22–26. [PubMed: 18822366]

Jiang R, Bush JO, Lidral A. Development of the upper lip: morphogenetic and molecular mechanisms. Dev Dyn. 2006; 235:1152–1166. [PubMed: 16292776]

Jones, KL. Smith's recognizable patterns of human malformation. 6th. Philadelphia: Elsevier; 2006.

Kahlem P, Sultan M, Herwig R, Steinfath M, Balzereit D, Eppens B, Saran NG, Pletcher MT, South ST, Stetten G, Lehrach H, Reeves RH, Yaspo ML. Transcript level alterations reflect gene dosage effects across multiple tissues in a mouse model of Down syndrome. Genome Res. 2004; 14:1258–1267. [PubMed: 15231742]

Kisling, E. Cranial morphology in Down's syndrome: a comparative roentgencephalometric study in adult males. Copenhagen: Orthodontic Department, Royal Danish Dental College; 1966.

Klingenberg C, McIntyre G. Geometric morphometrics of developmental instability: analyzing patterns of fluctuating asymmetry with Procrustes methods. Evolution. 1998; 52:1363–1375.

Klingenberg CP, Barluenga M, Meyer A. Shape analysis of symmetric structures: quantifying variation among individuals and asymmetry. Evolution. 2002; 56:1909–1920. [PubMed: 12449478]

Klingenberg CP, Wetherill L, Rogers J, Moore E, Ward R, Autti-Ramo I, Fagerlund A, Jacobson SW, Robinson LK, Hoyme HE, et al. Prenatal alcohol exposure alters the patterns of facial asymmetry. Alcohol. 2010; 44:649–657. [PubMed: 20060678]

Klingenberg CP. MorphoJ: an integrated software package for geometric morphometrics. Mol Ecol Resour. 2011; 11:353–357. [PubMed: 21429143]

Korbel JO, Tirosh-Wagner T, Urban AE, Chen XN, Kasowski M, Dai L, Grubert F, Erdman C, Gao MC, Lange K, et al. The genetic architecture of Down syndrome phenotypes revealed by high-resolution analysis of human segmental trisomies. Proc Natl Acad Sci USA. 2009; 106:12031–12036. [PubMed: 19597142]

Liu B, Rooker SM, Helms JA. Molecular control of facial morphology. Semin Cell Dev Biol. 2010; 21:309–313. [PubMed: 19747977]

Livshits G, Kobyliansky E. Fluctuating asymmetry as a possible measure of developmental homeostasis in humans: a review. Hum Biol. 1991; 63:441–466. [PubMed: 1889795]

Makino T, McLysaght A. Ohnologs in the human genome are dosage balanced and frequently associated with disease. Proc Natl Acad Sci USA. 2010; 107:9270–9274. [PubMed: 20439718]

Marcucio RS, Cordero DR, Hu D, Helms J. Molecular interactions coordinating the development of the forebrain and face. Dev Biol. 2005; 284:48–61. [PubMed: 15979605]

Megarbane A, Ravel A, Mircher C, Sturtz F, Grattau Y, Rethore MO, Delabar JM, Mobley WC. The 50th anniversary of the discovery of trisomy 21: the past, present, and future of research and treatment of Down syndrome. J Med Genet. 2009; 11:611–616.

Naugler CT, Ludman MD. Fluctuating asymmetry and disorders of developmental origin. Am J Med Genet. 1996; 66:15–20. [PubMed: 8957504]

Palmer, A., editor. Fluctuating asymmetry analysis: a primer. New York: Springer; 1994. p. 335-364.

Palmer A, Strobeck C. Fluctuating asymmetry as a measure of developmental stability: implications of non-normal distributions and power of statistical tests. Acta Zool Fennica. 1992; 191:57–72.

Palmer, A.; Strobeck, C., editors. Fluctuating asymmetry analyses revisited. New York: Oxford University Press; 2003. p. 279-319.

Palmer AR, Strobeck C. Fluctuating asymmetry: measurement, analysis, patterns. Ann Rev Ecol Syst. 1986; 17:391–421.

Parsons T, Ryan TM, Reeves RH, Richtsmeier JT. Microstructure of trabecular bone in a mouse model for Down syndrome. Anat Rec (Hoboken). 2007; 290:414–421. [PubMed: 17514765]

Reeves RH, Baxter LL, Richtsmeier JT. Too much of a good thing: mechanisms of gene action in Down syndrome. Trends Genet. 2001; 17:83–88. [PubMed: 11173117]

Richtsmeier, JT.; Lele, S.; Cole, TM, III. An invariant approach to the study of fluctuating asymmetry: developmental instability in a mouse model for Down syndrome. In: Slice, D., editor. Modern morphometrics in physical anthropology. New York: Kluwer Academic/Plenum Publishers Series; 2005. p. 187-212.

Roper RJ, VanHorn JF, Cain CC, Reeves RH. A neural crest deficit in Down syndrome mice is associated with deficient mitotic response to Sonic hedgehog. Mech Dev. 2009; 126:212–219. [PubMed: 19056491]

Rueda N, Flórez J, MartInez-Cue C. Mouse models of Down syndrome as a tool to unravel the causes of mental disabilities. Neural Plast. 2012; 2012:1–26.

Schmidt JL, Cole TM III, Silcox MT. A landmark-based approach to the study of ear ossicles using ultra-high-resolution X-ray computed tomography data. Am J Phys Anthropol. 2011; 145:665–671. [PubMed: 21732321]

Shapiro B. Prenatal dental anomalies in Mongolism: Comments on the Basis and Implications of variability. Ann NY Acad Sci. 1970; 171:562–577.

Shapiro B. Amplified developmental instability in Down's syndrome. Ann Hum Genet. 1975; 38:429–437. [PubMed: 127546]

Shapiro B. Down syndrome—a disruption of homeostasis. Am J Med Genet. 1983; 14:241–269. [PubMed: 6220605]

Shapiro BL. Development of human autosomal aneuploid phenotypes (with an emphasis on Down syndrome). Acta Zool Fennica. 1992; 191:97–105.

Shapiro BL, Gorlin RJ, Redman RS, Bruhl HH. The palate and Down's syndrome. N Engl J Med. 1967; 276:1460–1463. [PubMed: 4226066]

Szabo-Rogers HL, Geetha-Loganathan P, Nimmagadda S, Fu KK, Richman JM. FGF signals from the nasal pit are necessary for normal facial morphogenesis. Dev Biol. 2008; 318:289–302. [PubMed: 18455717]

Townsend GC. Fluctuating dental asymmetry in Down's syndrome. Aust Dent J. 1983; 28:39–44. [PubMed: 6222728]

Valeri CJ, Cole TM III, Lele S, Richtsmeier JT. Capturing data from three-dimensional surfaces using fuzzy landmarks. Am J Phys Anthropol. 1998; 107:113–124. [PubMed: 9740305]

Veitia RA, Bottani S, Birchler JA. Cellular reactions to gene dosage imbalance: genomic, transcriptomic and proteomic effects. Trends Genet. 2008; 24:390–397. [PubMed: 18585818]

Waddington, CH. The strategy of the genes. London: George Allen & Unwin; 1957.

Weinberg SM, Naidoo S, Govier DP, Martin RA, Kane AA, Marazita ML. Anthropometric precision and accuracy of digital three-dimensional photogrammetry: comparing the Genex and 3dMD imaging systems with one another and with direct anthropometry. J Craniofac Surg. 2006; 17:477–483. [PubMed: 16770184]

Willmore KE, Klingenberg CP, Hallgrímsson B. The relationship between fluctuating asymmetry and environmental variance in rhesus macaque skulls. Evolution. 2005; 59:898–909. [PubMed: 15926699]

Willmore KE, Zelditch ML, Young N, Ah-Seng A, Lozanoff S, Hallgrímsson B. Canalization and developmental stability in the Brachyrrhine mouse. J Anat. 2006; 208:361–372. [PubMed: 16533318]

Wiseman FK, Alford KA, Tybulewicz VL, Fisher EM. Down syndrome—recent progress and future prospects. Hum Mol Genet. 2009; 18:R75–R83. [PubMed: 19297404]

Wong JY, Oh AK, Ohta E, Hunt AT, Rogers GF, Mulliken JB, Deutsch CK. Validity and reliability of craniofacial anthropometric measurement of 3D digital photogrammetric images. Cleft Palate Craniofac J. 2008; 45:232–239. [PubMed: 18452351]

Wyganowska-Świątkowska M, Przystańska A. The Meckel's cartilage in human embryonic and early fetal periods. Anat Sci Int. 2011; 86:98–107. [PubMed: 20799009]

Young NM, Chong JH, Hu D, Hallgrímsson B, Marcucio RS. Quantitative analyses link modulation of sonic hedgehog signaling to continuous variation in facial growth and shape. Development. 2010; 137:3405–3409. [PubMed: 20826528]

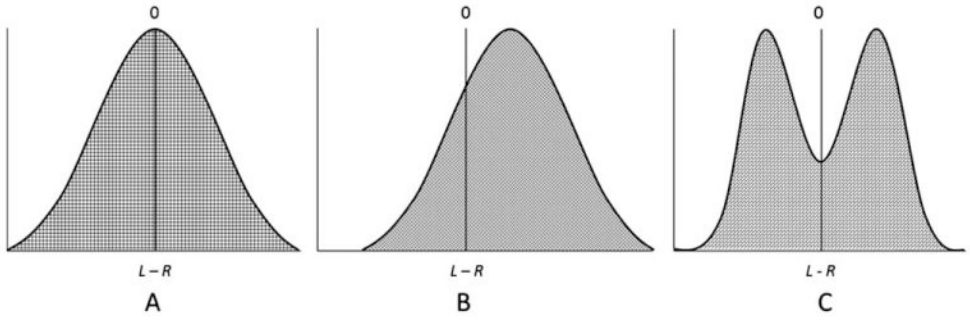

Fig. 1.

Types of asymmetry distributions. Asymmetry is characterized by the distribution of asymmetry values for particular characters in a sample (adapted from Palmer and Strobeck, 1986). Asymmetry is quantified as the signed difference between right and left sides (*L–R*) for a hypothetical characteristic of interest. (**A**) Fluctuating asymmetries deviate from perfect symmetry and are small and randomly distributed on each side so that the distribution of *L–R* values is unimodal and centered at zero. This definition assumes an underlying ideal form of perfect symmetry (i.e., $L-R=0$). (**B**) Directionally asymmetric measurements are consistently larger on one side than on the other side and the mean value is non-zero (i.e., $L-R\neq 0$). (**C**) Antisymmetry refers to measurements that are asymmetric but these measurements can be larger on one side in some individuals and larger on the other side in different individuals, which causes the distribution of signed differences between the left and right side to be bimodal.

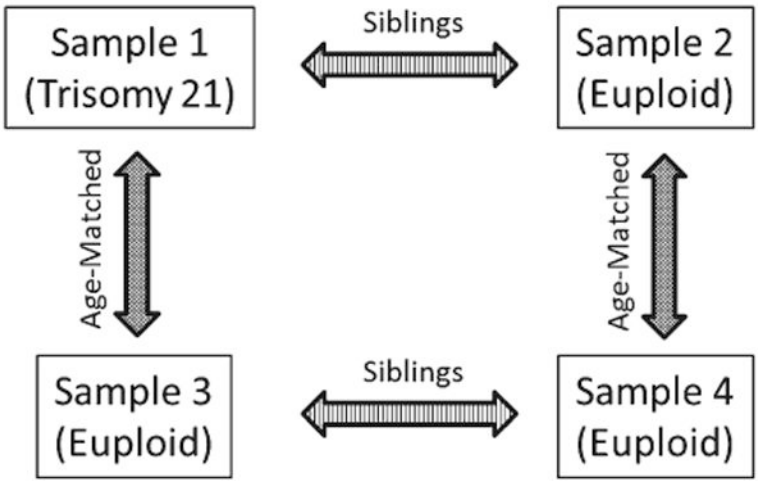

Fig. 2.

Four-sample study design. Four samples are depicted: (**A**) sample 1—individuals with Down syndrome, (**B**) sample 2—euploid biological siblings of individuals with Down syndrome, (**C**) sample 3—euploid individuals who are age matched to sample 1, and (**D**) sample 4—euploid individuals who are age-matched to sample 2 and who have a single sibling in sample 3. Sample 1 is age-matched to sample 3. Sample 2 is age-matched to sample 4. This four sample designs allow us to estimate the number of differences in FA between biological siblings (i.e., samples 1 and 2, and samples 3 and 4) and to subtract away differences we expect to find between unaffected siblings (estimated from samples 3 and 4) to determine how trisomy is altering developmental stability in the Down syndrome face.

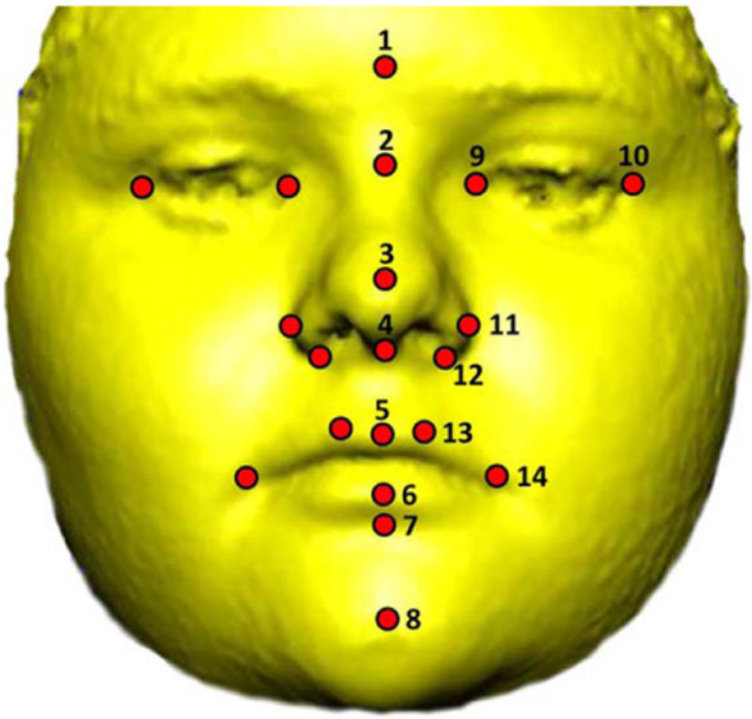

Fig. 3.

Soft-tissue facial landmarks. The 3dMDpatient (v4.0) software was used to record the three-dimensional coordinates of 20 standard landmarks (circles) from each image on two separate occasions. Eight medial and six bilateral landmarks were used in this study: 1) gonion (g), 2) nasion (n), 3) pronasale (prn), 4) subnasale (sn), 5) labiale superius (ls), 6) labiale inferius (li), 7) sublabiale (Sl), 8) pogonion (SPg), 9) endocanthion (en), 10) exocanthion (ex), 11) alar curvature (ac), 12) subalare (sbal), 13) crista philtra landmark (cpl), and 14) chelion (ch). Anatomical definitions of landmarks are adapted from Farkas (1991), and landmark definitions can be found at http://geta-head.psu.edu/. Written consent from the parent or guardian was acquired to publish facial images.

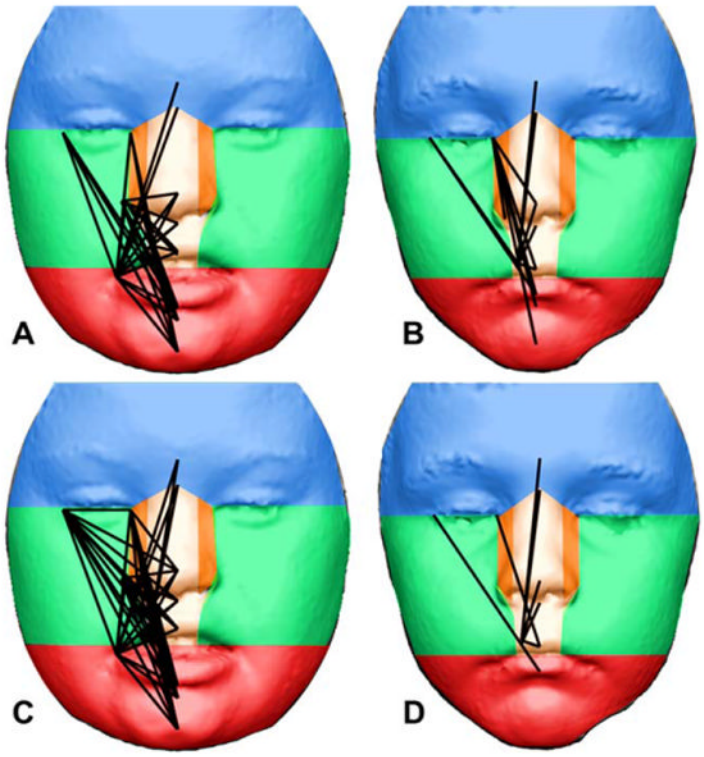

Fig. 4.

Linear distances that exhibit significantly different FA between sibling pairs overlain upon faces divided into developmental precursors. Significantly different linear distances from EDMA two-sample analyses of FA are depicted as black lines upon faces that have been divided into developmental facial prominences that give rise to these regions: frontal prominence (blue), paired mandibular prominences (green), paired lateral nasal prominences (orange), paired medial nasal prominences (tan), and the mandibular prominence (red). Based on the difference (*L–R*) EDMA FA analysis, a total of 35 linear distances (56%) exhibit significantly different FA between the DS and DS sibling sample (**A**), whereas only 13 linear distances (21%) exhibit significantly different FA between typical sibling samples (**C**). Based on the ratio (Ln *(L/R)*) EDMA FA analysis, a total of 48 linear distances (76%) exhibit significantly different FA between the DS and DS sibling sample (**B**), whereas only seven linear distances (11%) exhibit significantly different FA between typical sibling samples (**D**). Notably, every single linear distance exhibiting significantly different FA between the DS and DS sibling samples has a larger magnitude of FA in the DS sample for each of the two bootstrap analyses. Written consent from the parent or guardian was acquired to publish facial images.

Table 1
Average amount of facial FA across samples

Fluctuating asymmetry across samples				
	Sample 1 (DS)	**Sample 2 (DS sibs)**	**Sample 3 (typical sibs)**	**Sample 4 (typical sibs)**
Difference (L–R)	1.1123	0.7298	0.7232	0.7955
DS% relative increase	N/A	152.41%	153.80%	139.82%
Ratio Ln(*L*/*R*)	0.0363	0.0221	0.0226	0.0238
DS % relative increase	N/A	164.25%	160.62%	152.52%

For each sample the amount of average FA is shown for both the difference (*L*–*R*) and ratio (Ln(*L*/*R*)) analysis for all 63 bilateral paired linear distances across the face. The relative increase for the DS sample (i.e., the amount of fluctuating asymmetry in DS divided by the amount of fluctuating asymmetry of other samples) is also shown.

Table 2

Frequency that each linear distance exhibiting significantly different FA crosses each developmental region of the face for each two-sample bootstrap comparison

	Frequency that facial regions are crossed				
	Frontal	**Maxillary**	**Lateral Nasal**	**Medial Nasal**	**Mandibular**
Difference (L–R)					
Sample 1/2	1	15	7	27	25
Sample 3/4	1	2	6	12	3
Difference	0	13	1	15	22
Total possible	9	21	30	42	30
Percentage	0.00	61.90	3.33	35.71	73.33
Ratio Ln(*L/R*)					
Sample 1/2	2	21	14	34	30
Sample 3/4	1	1	1	7	1
Difference	1	20	13	27	29
Total possible	9	21	30	42	30
Percentage	11.11	95.24	43.33	64.29	96.67